PHOTONICS Research

Photonic chip-based optical frequency division with PZT-integrated soliton microcombs

Ruxuan Liu,[1] Mark W. Harrington,[2] Shuman Sun,[1] Fatemehsadat Tabatabaei,[1] Samin Hanifi,[1] Meiting Song,[2] Kaikai Liu,[2] Jiawei Wang,[2] Haoran Chen,[1] Zijiao Yang,[1,3] Beichen Wang,[1] Fateme Majdi,[1] Paul A. Morton,[4] Karl D. Nelson,[5] Steven M. Bowers,[1] Andreas Beling,[1] Ryan Q. Rudy,[6] Iain M. Kierzewski,[6] Daniel J. Blumenthal,[2,7] and Xu Yi[1,3,8]

[1]Department of Electrical and Computer Engineering, University of Virginia, Charlottesville, Virginia 22904, USA
[2]Department of Electrical and Computer Engineering, University of California Santa Barbara, Santa Barbara, California 93016, USA
[3]Department of Physics, University of Virginia, Charlottesville, Virginia 22904, USA
[4]Infleqtion, Louisville, Colorado 80027, USA
[5]Honeywell Aerospace Technologies, Plymouth, Minnesota 55441, USA
[6]DEVCOM Army Research Laboratory, Adelphi, Maryland 20783, USA
[7]e-mail: danb@ucsb.edu
[8]e-mail: yi@virginia.edu

Received 23 July 2025; revised 21 October 2025; accepted 22 October 2025; posted 10 November 2025 (Doc. ID 574352); published 30 January 2026

Optical frequency division (OFD) produces low-noise microwave and millimeter-wave (mmWave) signals by transferring the exceptional stability of optical references to electronic frequency domains. Recent developments in integrated optical references and soliton microcombs have paved the way for miniaturizing OFD oscillators to chip scale. Critical to this realization is a rapid tunable frequency comb that is stabilized to the optical references, thereby coherently linking optical and electronic frequencies. In this work, we advance the on-chip OFD technology using an integrated high-speed lead zirconate titanate (PZT) stress-optic actuator on the SiN soliton microcomb resonator. The integrated PZT actuator tunes the resonance frequency of the soliton-generating microresonator with a bandwidth exceeding 10s MHz and thus adjusts the soliton repetition rate. Optical frequency division and low-noise mmWave generation are demonstrated by feedback control of the soliton repetition rate through the integrated PZT-actuator, and the soliton microcomb is stabilized to a pair of reference lasers that are locked to an integrated 4 m SiN coil reference cavity. Our approach provides a fast, versatile, and integrated control mechanism for OFD oscillators and their applications in advanced communications, sensing, and precise timing.

https://doi.org/10.1364/PRJ.574352

1. INTRODUCTION

Optical frequency division (OFD) is able to transfer the exceptional fractional stability from stable optical references to electronic frequencies through the use of optical frequency combs (OFCs) [1]. It has set the phase noise record in microwave and millimeter-wave (mmWave) regimes [2–5], with the potential to revolutionize many applications, including communications, sensing, and precise timing [6–8]. Very recently, OFD technology has been transitioning to chip scale thanks to developments in integrated optical references [9–13] and soliton microresonator-based frequency combs (microcombs) [14–18], and is rapidly advancing the spectral purity of integrated microwave and millimeter-wave oscillators [19–25].

The implementation of OFD relies upon the feedback control of an optical frequency comb, which stabilizes the comb to the optical reference and provides a coherent link between optical and electronic frequencies. A direct, rapid tuning mechanism for the frequency comb cavity is thus critical to OFD oscillators. The miniaturization of OFD oscillators offers a unique opportunity to enable a much faster control on the frequency comb than that in the bulk OFD systems, as the bandwidth of electronics and mechanics typically increases with the decrease of device dimension. Indeed, integrated stress-optics actuators, such as lead zirconate titanate (PZT) actuators [26–30], have reached a modulation bandwidth of 10s MHz [31,32] and are readily integrated with high-Q optical microcavities [30,33–35]. Electro-optic modulators provide even higher tuning speed [36,37]. However, their integration into OFD oscillators has not been explored in previous on-chip OFD demonstrations, where the microcomb was tuned either

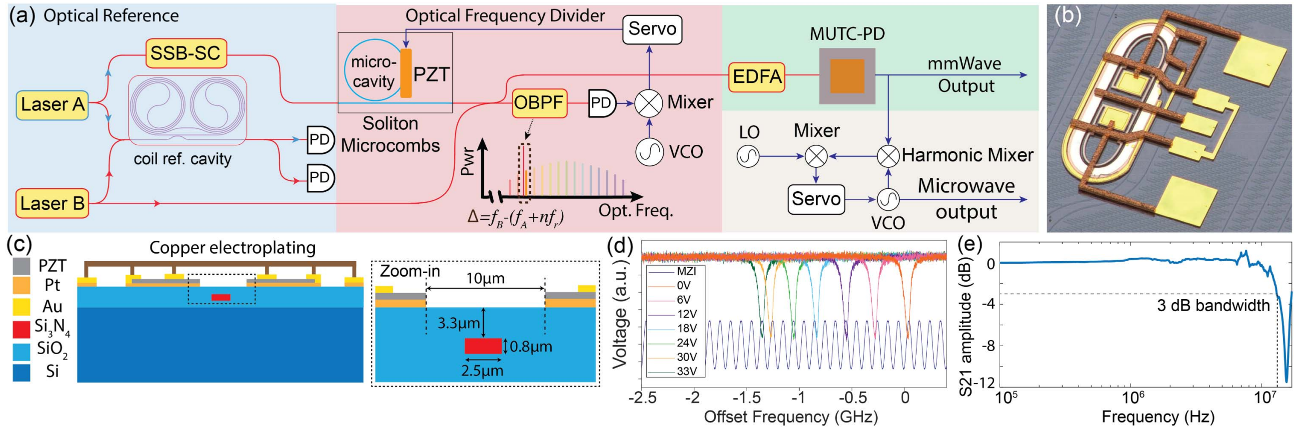

Fig. 1. Conceptual illustration of OFD with PZT actuators and characterization of PZT-integrated microresonator. (a) Simplified illustration for the OFD experimental setup. A pair of lasers at 1550 nm (laser A) and 1600 nm (laser B) is stabilized to an integrated 4 m SiN coil reference cavity using the PDH locking technique. A fast-tuning sideband of laser A, created by modulating a single-sideband suppressed carrier modulator (SSB-SC), is used to generate the soliton microcomb in the PZT-integrated SiN microcavity. To implement the OFD, the N-th comb line is phase locked to laser B by feedback control of the soliton repetition rate using the integrated PZT actuator. The soliton microcomb is then amplified and photodetected on a high-speed MUTC-PD to generate low-noise mmWave. Erbium-doped fiber amplifier (EDFA), voltage controlled oscillators (VCOs), optical bandpass filter (OBPF), and photodiodes (PDs) are used in the experiment. (b) Image of a typical PZT-integrated SiN microcomb resonator. (c) Illustrative cross-section of the SiN waveguide and PZT actuator layers. Not drawn to scale. Zoomed-in panel shown on the right. (d) Microresonator resonance frequency tuning versus bias voltage on PZT. An MZI with 100 MHz period is used for frequency calibration. (e) Frequency response (S21) to characterize the bandwidth of the PZT actuator.

by the frequency of its pump laser [4,19,20,24,25], or passively using laser injection locking [21,23,38–40].

In this work, we demonstrate optical frequency division and low-noise mmWave generation by using a PZT-integrated soliton microcomb [Fig. 1(a)]. The PZT-based stress-optics actuator is directly integrated on the SiN soliton microcomb cavity [Fig. 1(b)], and it can tune the microcavity resonance frequency and thus the repetition rate of the soliton microcomb. The actuator has a 3 dB bandwidth of 10s MHz, and the speed of the OFD feedback control is limited by the electronics of the PID loop. The PZT-integrated soliton microcomb is stabilized to a pair of reference lasers that are PDH locked to an integrated SiN 4 m coil reference cavity [12]. 109.5 GHz mmWave signal is generated by photodetecting the soliton microcombs with a modified uni-traveling carrier photodiode (MUTC-PD) [41,42]. The phase noise at 10 kHz offset frequency reaches −114 dBc/Hz, which is equivalent to −135 dBc/Hz when the carrier frequency is scaled to 10 GHz. The phase noise performance aligns well with our previous record-setting OFD demonstrations [19,23] at 100s GHz carrier frequency, and is primarily limited by the optical reference and mmWave phase noise measurement method.

2. RESULTS

A PZT-integrated Si_3N_4 racetrack-shaped microresonator is used for soliton microcomb generation. The resonator has a cross-section of 2.5 μm width by 0.8 μm height, a free spectral range (FSR) of 109.5 GHz, and an intrinsic (loaded) quality factor of 3.85×10^6 (2.87×10^6). The SiN resonator has a top oxide cladding layer of 3.3 μm. The piezo-electric (PZT, lead zirconate titanate) actuator is then fabricated on top of the oxide cladding. Details of the PZT actuator fabrication have been described elsewhere [35]. A side-view of the PZT actuator structure is shown in Fig. 1(c). For the SiN waveguide of 800 nm thickness, the optical mode is well confined in the SiN core, and the PZT actuator will not impact the Q-factor of the microresonator.

The modulation property of the PZT-integrated microresonator is characterized and presented in Figs. 1(d) and 1(e). The PZT actuator is tuned by applying an electrical field using a DC probe, and the waveguide refractive index is changed by the strain induced through the piezoelectric effect. The frequency shift of the microresonator in response to the applied DC voltage on the PZT probe is shown in Fig. 1(d). A tuning coefficient of 43.7 MHz/V is observed, with the accuracy limited by the relative frequency drift of the resonator and the calibrating Mach–Zehnder interferometer (MZI) due to environmental temperature fluctuation. The small-signal electrical-to-optical modulation response S21 is measured with a vector network analyzer (VNA). The small signal is sent to the PZT actuator, and the transmission of the microresonator is detected on a photodiode. To obtain the information of the resonance frequency, a frequency to amplitude conversion is required, which is achieved by detuning the probe laser frequency to the full width at half-maximum (FWHM) point of the microcavity resonance. The S21 magnitude is shown in Fig. 1(e). A 3 dB bandwidth is measured to be around 13 MHz. The small-signal measurement is sensitive to the relative detuning of the probe laser and the resonator frequency. It should be noted that a resonance dip is observed around 20 MHz frequency, which likely comes from the electronic circuits instead of the PZT itself. Nevertheless, this measured bandwidth far exceeds the servo bandwidth achieved in OFD [19,20,25], and will not be a limiting factor of the OFD bandwidth.

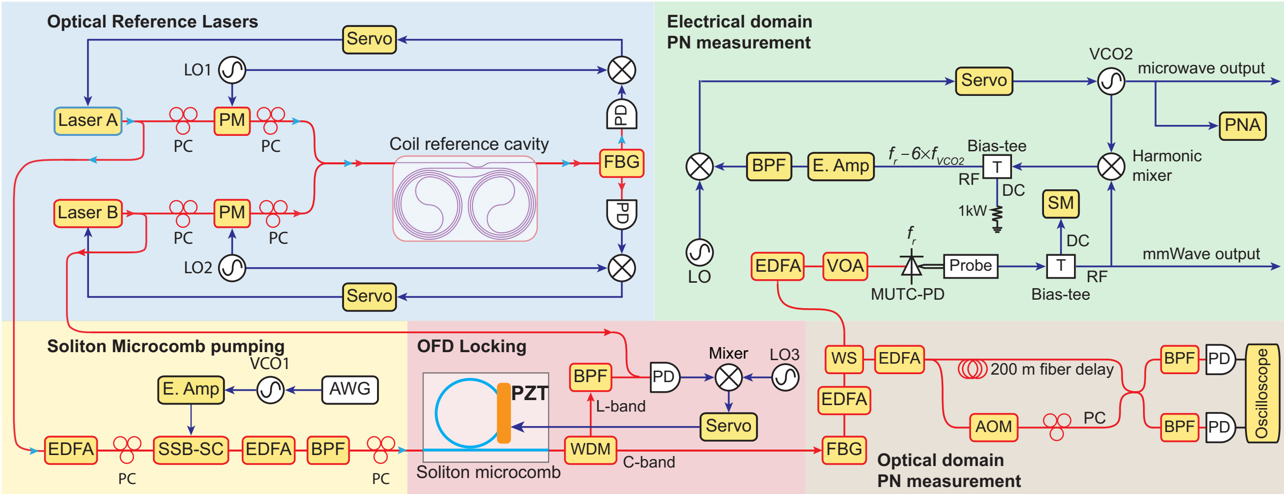

Fig. 2. Full experimental setup. The PZT-OFD oscillator outputs a stable mmWave signal at 110 GHz. The mmWave phase noise is characterized by a dual-tone delayed self-heterodyne interferometry method (optical domain) and an mmWave to microwave frequency division (mmFD) method (electrical domain). In the electrical method, the mmFD down-converts the carrier frequency from 110 GHz to 18 GHz for direct measurement on a phase noise analyzer (PNA). Polarization controllers (PCs), phase modulators (PMs), bandpass filters (BPFs), fiber-Bragg grating (FBG) filters, wavelength division multiplexer (WDM), line-by-line waveshaper (WS), electrical amplifier (E. Amp), source meter (SM), and acoustic-optic modulator (AOM) are used in the experiment.

The PZT-actuated soliton microcomb is then applied to demonstrate optical frequency division and low-noise mmWave generation. The full schematic of the experimental setup is shown in Fig. 2. In our OFD demonstration, the oscillator derives its stability from two optical references near 1550 nm ($f_A = 193.5$ THz) and 1600 nm ($f_B = 187.4$ THz), which are both stabilized to a common integrated 4 m SiN coil reference cavity [12] through the Pound–Drever–Hall (PDH) locking technique. The coil reference cavity has an intrinsic (loaded) Q-factor of $6.6 \times 10^7 (4.6 \times 10^7)$ at 1550 nm. A modulation sideband of reference laser A directly drives the soliton microcomb [43] and serves as the zeroth comb line, with the comb line frequency at $f_0 = f_A + f_{\mathrm{VCO1}}$. The reference lasers and soliton generation have been described elsewhere [19,23]. To implement OFD, the second reference laser at 1600 nm is photomixed with the comb line at $N = -54$, and their beatnote is used to phase lock the N-th comb line to the reference laser by feedback control of soliton repetition rate through tuning the PZT actuator. No optical amplifier is used to amplify the power of the comb line for OFD locking. When phase locked, the frequency of the N-th comb line will be $f_N = f_B + f_{\mathrm{LO3}}$, which also equals $f_N = f_0 + N \times f_r = f_A + f_{\mathrm{VCO1}} + N \times f_r$, where f_r is the repetition rate of the soliton. An optical frequency division is thus achieved, as $f_r = (f_B - f_A)/N + (f_{\mathrm{LO3}} - f_{\mathrm{VCO1}})/N$. In our system, the phase noise of the VCO1 and LO3 is much lower than that of the two optical reference lasers, and thus the phase noise of soliton repetition rate is dominated by the divided optical references: $S_r = (S_A + S_B)/N^2$, where S_r, S_A, and S_B are the phase noise of soliton repetition rate, reference laser A, and reference laser B, respectively. This configuration achieves a frequency division ratio of 54 (from 6 THz to 110 GHz), offering a phase noise reduction of $54^2 = 2916 \approx 35$ dB (in log scale). The optical spectra of the soliton microcomb and reference lasers are shown in Fig. 3(a).

The phase-stabilized PZT-controlled solitons are then amplified and sent to a high-speed MUTC photodiode to generate a low-noise mmWave signal at 110 GHz carrier frequency [41]. To measure the phase noise of 110 GHz, two methods are utilized. For offset frequencies below 30 kHz, an mmWave to microwave frequency division (mmFD) [19] is applied to down-convert the carrier frequency from 110 GHz to 18 GHz, whose phase noise and electrical spectra [Fig. 3(b)] can be directly measured on a phase noise analyzer [19]. The measured phase noise is then scaled back to 110 GHz to give an upper bound limit of the mmWave phase noise. The mmFD method has a locking bandwidth of roughly 282 kHz. Beyond 30 kHz offset frequency, the phase noise is measured optically using a dual-tone delayed self-heterodyne interferometry method [19,44] (optical method). The combined phase noise is shown in Fig. 3(c), with carrier frequency scaled to 110 GHz (native) and 10 GHz. To validate OFD, the phase noise of the phase difference between the reference lasers is measured with the optical method and is presented in Fig. 4. The phase noise of the soliton repetition rate measured using the same optical method is also shown in Fig. 4, and matches well with that of the OFD projection (phase noise of reference lasers −35 dB), which validates the PZT-enabled OFD. It should be noted that the optical method overestimates phase noise in the low-offset frequency due to slow drifts in optical interferometry, which has been shown previously [19].

The phase noise of the generated mmWave is very low for an integrated oscillator. At 10 kHz offset, the oscillator has a phase noise of −114 dBc/Hz, which is equivalent to −135 dBc/Hz when the carrier frequency is scaled down to 10 GHz. This result is comparable to our non-PZT integrated OFD oscillator

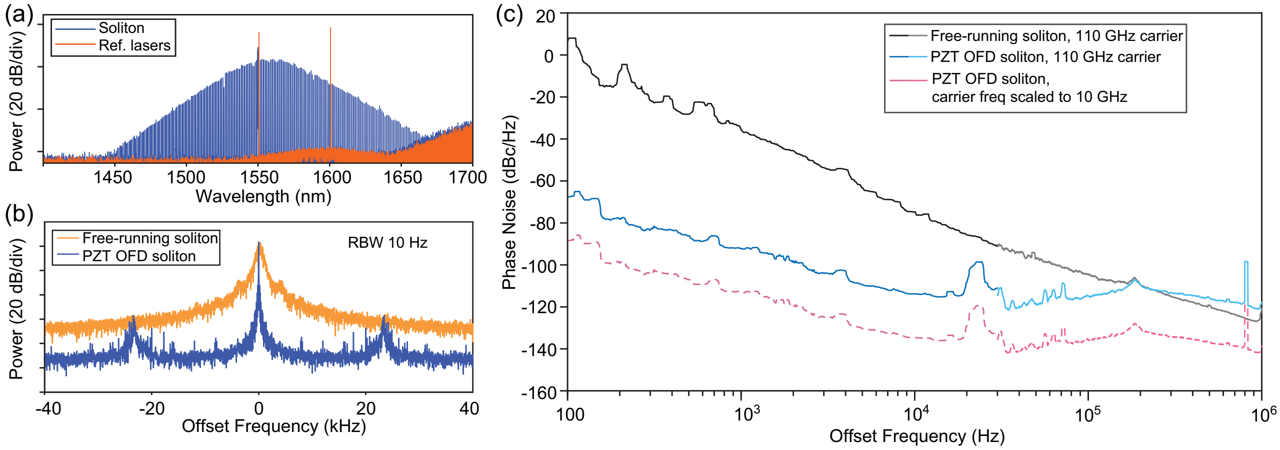

Fig. 3. Results of optical frequency division using PZT-integrated soliton microcomb. (a) Optical spectra of soliton microcomb (blue) and a pair of reference lasers (orange). (b) Electrical spectra of the mmWave output after mmWave to microwave frequency division for free running soliton (orange) and PZT-integrated OFD soliton (blue). (c) Phase noise characterization of free-running soliton (black) and integrated-PZT OFD soliton (blue). The pink trace shows the phase noise of PZT OFD soliton when the carrier frequency is scaled down to 10 GHz.

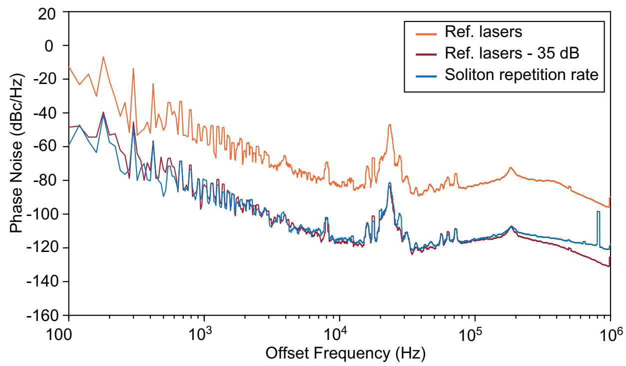

Fig. 4. Validation of optical frequency division. Phase noise of the soliton repetition rate (blue) and the phase difference between reference lasers (orange) are shown. The phase noise of the soliton repetition rate matches well with the OFD projection, which is the phase noise of reference lasers −35 dB (red). Phase noise presented in this figure is measured with dual-tone delayed self-heterodyne interferometry method.

reported previously [19]. The phase noise of both oscillators is primarily limited by the reference lasers. Also, the mmFD phase noise measurement at 100s GHz contributes excess phase noise. Other OFD oscillators [23] could have better phase noise performance due to lower reference laser noise. Surprisingly, the PZT OFD servo bandwidth is only 200 kHz, which is significantly lower than the bandwidth of PZT itself. We believe that this is limited by the servo loop itself, and could be dramatically improved in the future when electronics and feedback loop are specifically designed for PZT-enabled OFD.

3. SUMMARY

In summary, we have demonstrated optical frequency division and low-noise mmWave generation using PZT-integrated soliton microcombs. The integrated PZT actuator contributes a new rapid tuning mechanism in OFD oscillators and simplifies its implementation. In our system, only two reference lasers are used to both generate the solitons and implement OFD. No additional laser is required to pump the soliton and tune its repetition rate, which is much improved from the initial integrated OFD demonstration [19,20]. Compared with the passive locking OFD method, e.g., Kerr OFD [21,23,39], the PZT OFD does not require fine frequency alignment of the reference lasers and microcombs. Finally, in our demonstration, in addition to optical frequency division, the entire soliton microcomb is fully phase stabilized to the reference lasers, as two comb lines, the zeroth line and N-th line, are stabilized to the reference lasers. This eliminates any free-running parameter in the frequency of the microcomb, and thus achieves full stabilization to a reference cavity. Recent demonstration of heterogeneously integrated soliton microcombs and MUTC photodiodes [45] can provide a path for further integration of OFD oscillators.

Funding. Defense Advanced Research Projects Agency (HR0011-22-2-0008, N660012424000); National Science Foundation (2023775).

Acknowledgment. The authors acknowledge M. Woodson and S. Estrella from Freedom Photonics for the MUTC PD fabrication, Ligentec for SiN microresonator fabrication, and gratefully acknowledge DARPA GRYPHON (HR0011-22-2-0008), DARPA NaPSAC (N660012424000) and National Science Foundation (2023775), and ARL acknowledges W911NF2220056.

Author Contributions. X.Y. and R.L designed the experiments. R.L, F.T., and S.H. performed the oscillator measurements. R.R. and I.K. fabricated the PZT actuators, R.L. and M.W.H characterized the PZT. J.S.M. and A.B. designed and fabricated the integrated photodiodes. S.S., Z.Y., and B.W. designed the integrated photonic circuits. R.L and

X.Y. analyzed the experimental results. X.Y., D.J.B., R.R., A.B., S.M.B., P.A.M., and K.D.N. supervised and led the scientific collaboration. All authors participated in preparing the manuscript.

Disclosures. The authors declare no conflicts of interest. The views and conclusions contained in this document are those of the authors and should not be interpreted as representing official policies of DARPA or the U.S. Government.

Data Availability. Data for Figs. 1, 3, and 4 can be accessed [46].

REFERENCES

1. T. M. Fortier, M. S. Kirchner, F. Quinlan, *et al.*, "Generation of ultrastable microwaves via optical frequency division," Nat. Photonics **5**, 425–429 (2011).
2. X. Xie, R. Bouchand, D. Nicolodi, *et al.*, "Photonic microwave signals with zeptosecond-level absolute timing noise," Nat. Photonics **11**, 44–47 (2017).
3. T. Nakamura, J. Davila-Rodriguez, H. Leopardi, *et al.*, "Coherent optical clock down-conversion for microwave frequencies with 10^{-18} instability," Science **368**, 889–892 (2020).
4. T. Tetsumoto, T. Nagatsuma, M. E. Fermann, *et al.*, "Optically referenced 300 GHz millimetre-wave oscillator," Nat. Photonics **15**, 516–522 (2021).
5. J. Li and K. Vahala, "Small-sized, ultra-low phase noise photonic microwave oscillators at X-Ka bands," Optica **10**, 33–34 (2023).
6. S. Koenig, D. Lopez-Diaz, J. Antes, *et al.*, "Wireless sub-THz communication system with high data rate," Nat. Photonics **7**, 977–981 (2013).
7. P. Ghelfi, F. Laghezza, F. Scotti, *et al.*, "A fully photonics-based coherent radar system," Nature **507**, 341–345 (2014).
8. D. Long and F. Ulaby, *Microwave Radar and Radiometric Remote Sensing* (Artech, 2015).
9. H. Lee, M.-G. Suh, T. Chen, *et al.*, "Spiral resonators for on-chip laser frequency stabilization," Nat. Commun. **4**, 2468 (2013).
10. W. Jin, Q.-F. Yang, L. Chang, *et al.*, "Hertz-linewidth semiconductor lasers using CMOS-ready ultra-high-*Q* microresonators," Nat. Photonics **15**, 346–353 (2021).
11. B. Li, W. Jin, L. Wu, *et al.*, "Reaching fiber-laser coherence in integrated photonics," Opt. Lett. **46**, 5201–5204 (2021).
12. K. Liu, N. Chauhan, J. Wang, *et al.*, "36 Hz integral linewidth laser based on a photonic integrated 4.0 m coil resonator," Optica **9**, 770–775 (2022).
13. J. Guo, C. A. McLemore, C. Xiang, *et al.*, "Chip-based laser with 1-hertz integrated linewidth," Sci. Adv. **8**, eabp9006 (2022).
14. T. Herr, V. Brasch, J. D. Jost, *et al.*, "Temporal solitons in optical microresonators," Nat. Photonics **8**, 145–152 (2014).
15. X. Yi, Q.-F. Yang, K. Y. Yang, *et al.*, "Soliton frequency comb at microwave rates in a high-*Q* silica microresonator," Optica **2**, 1078–1085 (2015).
16. V. Brasch, M. Geiselmann, T. Herr, *et al.*, "Photonic chip-based optical frequency comb using soliton Cherenkov radiation," Science **351**, 357–360 (2016).
17. T. J. Kippenberg, A. L. Gaeta, M. Lipson, *et al.*, "Dissipative Kerr solitons in optical microresonators," Science **361**, eaan8083 (2018).
18. A. L. Gaeta, M. Lipson, and T. J. Kippenberg, "Photonic-chip-based frequency combs," Nat. Photonics **13**, 158–169 (2019).
19. S. Sun, B. Wang, K. Liu, *et al.*, "Integrated optical frequency division for microwave and mmWave generation," Nature **627**, 540–545 (2024).
20. I. Kudelin, W. Groman, Q.-X. Ji, *et al.*, "Photonic chip-based low-noise microwave oscillator," Nature **627**, 534–539 (2024).
21. Y. Zhao, J. K. Jang, G. J. Beals, *et al.*, "All-optical frequency division on-chip using a single laser," Nature **627**, 546–552 (2024).
22. Y. He, L. Cheng, H. Wang, *et al.*, "Chip-scale high-performance photonic microwave oscillator," Sci. Adv. **10**, eado9570 (2024).
23. S. Sun, M. W. Harrington, F. Tabatabaei, *et al.*, "Microcavity Kerr optical frequency division with integrated SiN photonics," Nat. Photonics **19**, 637–642 (2025).
24. Q.-X. Ji, W. Zhang, A. Savchenkov, *et al.*, "Dispersive-wave-agile optical frequency division," Nat. Photonics **19**, 624–629 (2025).
25. X. Jin, Z. Xie, X. Zhang, *et al.*, "Microresonator-referenced soliton microcombs with zeptosecond-level timing noise," Nat. Photonics **19**, 630–636 (2025).
26. J. S. Pulskamp, R. G. Polcawich, R. Q. Rudy, *et al.*, "Piezoelectric PZT MEMS technologies for small-scale robotics and RF applications," MRS Bull. **37**, 1062–1070 (2012).
27. G. L. Smith, J. S. Pulskamp, L. M. Sanchez, *et al.*, "PZT-based piezoelectric mems technology," J. Am. Ceram. Soc. **95**, 1777–1792 (2012).
28. S. S. Bedair, J. S. Pulskamp, C. D. Meyer, *et al.*, "High-performance micromachined inductors tunable by lead zirconate titanate actuators," IEEE Electron Dev. Lett. **33**, 1483–1485 (2012).
29. J. S. Pulskamp, S. S. Bedair, R. G. Polcawich, *et al.*, "High-*Q* and capacitance ratio multilayer metal-on-piezoelectric RF MEMS varactors," IEEE Electron Dev. Lett. **35**, 871–873 (2014).
30. H. Tian, J. Liu, A. Attanasio, *et al.*, "Piezoelectric actuation for integrated photonics," Adv. Opt. Photonics **16**, 749–867 (2024).
31. N. Hosseini, R. Dekker, M. Hoekman, *et al.*, "Stress-optic modulator in triplex platform using a piezoelectric lead zirconate titanate (PZT) thin film," Opt. Express **23**, 14018–14026 (2015).
32. W. Jin, R. G. Polcawich, P. A. Morton, *et al.*, "Piezoelectrically tuned silicon nitride ring resonator," Opt. Express **26**, 3174–3187 (2018).
33. J. Liu, H. Tian, E. Lucas, *et al.*, "Monolithic piezoelectric control of soliton microcombs," Nature **583**, 385–390 (2020).
34. G. Lihachev, J. Riemensberger, W. Weng, *et al.*, "Low-noise frequency-agile photonic integrated lasers for coherent ranging," Nat. Commun. **13**, 3522 (2022).
35. J. Wang, K. Liu, M. W. Harrington, *et al.*, "Silicon nitride stress-optic microresonator modulator for optical control applications," Opt. Express **30**, 31816–31827 (2022).
36. C. Wang, M. Zhang, X. Chen, *et al.*, "Integrated lithium niobate electro-optic modulators operating at CMOS-compatible voltages," Nature **562**, 101–104 (2018).
37. Y. He, R. Lopez-Rios, U. A. Javid, *et al.*, "High-speed tunable microwave-rate soliton microcomb," Nat. Commun. **14**, 3467 (2023).
38. H. Taheri, A. B. Matsko, and L. Maleki, "Optical lattice trap for Kerr solitons," Eur. Phys. J. D **71**, 153 (2017).
39. G. Moille, J. Stone, M. Chojnacky, *et al.*, "Kerr-induced synchronization of a cavity soliton to an optical reference," Nature **624**, 267–274 (2023).
40. T. Wildi, A. Ulanov, N. Englebert, *et al.*, "Sideband injection locking in microresonator frequency combs," APL Photonics **8**, 120801 (2023).
41. B. Wang, J. S. Morgan, K. Sun, *et al.*, "Towards high-power, high-coherence, integrated photonic mmwave platform with microcavity solitons," Light Sci. Appl. **10**, 4 (2021).
42. W. Sun, Z. Chen, L. Li, *et al.*, "A chip-integrated comb-based microwave oscillator," Light Sci. Appl. **14**, 179 (2025).
43. J. R. Stone, T. C. Briles, T. E. Drake, *et al.*, "Thermal and nonlinear dissipative-soliton dynamics in kerr-microresonator frequency combs," Phys. Rev. Lett. **121**, 063902 (2018).
44. D. Kwon, C.-G. Jeon, J. Shin, *et al.*, "Reference-free, high-resolution measurement method of timing jitter spectra of optical frequency combs," Sci. Rep. **7**, 40917 (2017).
45. J. Gao, B. Wang, F. Tabatabaei, *et al.*, "Heterogeneous integration of a high-speed photodiode with microcavity solitons for on-chip mmWave generation," Optica **12**, 465–468 (2025).
46. https://doi.org/10.6084/m9.figshare.30407812.